

Supplementary Materials for

ETV7 is an essential component of a rapamycin-insensitive mTOR complex in cancer

Franklin C. Harwood, Ramon I. Klein Geltink, Brendan P. O'Hara, Monica Cardone, Laura Janke, David Finkelstein, Igor Entin, Leena Paul, Peter J. Houghton, Gerard C. Grosveld*

*Corresponding author. Email: gerard.grosveld@stjude.org

Published 12 September 2018, *Sci. Adv.* **4**, eaar3938 (2018)
DOI: 10.1126/sciadv.aar3938

The PDF file includes:

- Fig. S1. ETV7 is expressed in pediatric malignancies.
- Fig. S2. PI3K and PTK2 signaling and anti-p-tyr Western blot of cell lysate of vector and ETV7 mouse pre-B cells.
- Fig. S3. ETV7 expression in human pediatric tumor xenografts.
- Fig. S4. Sequence comparison of ETV6 and ETV7 PNT domains and the position of $\Delta 9$, $\Delta 27$, $\Delta 120/\Delta 115$, $\Delta 120/\Delta 159/+60$ mutations in the ETV7 PNT domain, and the KALK mutation in the ETV7 ETS domain.
- Fig. S5. mTOR localization and assembly.
- Fig. S6. Effects of mTOR inhibitors and mTORC3 loss on mTOR signaling.
- Fig. S7. Effect of ALK inhibition on p-AKT^{Ser473} and relative FK506-binding protein expression in Karpas-299 cells.
- Fig. S8. mTORC3 kinase is insensitive to Raptor or Rictor knockdown or Rictor knockout.
- Fig. S9. ERMS-specific markers in Ptch^{+/-}/ETV^{TG+/-} tumors are preserved in Ptch^{+/-}/ETV^{TG+/-} cell lines.
- Fig. S10. Whole phospho-p70S6K^{Thr389} and p70S6K Western blots relating to Figs. 1C and 5D.
- Table S1. Expression effects of ETV7.

Other Supplementary Material for this manuscript includes the following:

(available at advances.sciencemag.org/cgi/content/full/4/9/eaar3938/DC1)

- Movie S1 (.mp4 format). Induction of non-targeting ETV7shRNA in human DAOY medulloblastoma cells.
- Movie S2 (.mp4 format). Induction of targeting ETV7shRNA in human DAOY medulloblastoma cells.

Fig. S1. ETV7 is expressed in pediatric malignancies. Histograms of expression levels of ETV7 in (A) pediatric ALL (19) and (B) pediatric AML (18) using the Affymetrix U133Av2 array. The division of ETV7⁺ (red) and ETV7⁻ (green) tumors (relative expression value 200) was based on the hybridization level of ETV7 in non-ETV7 expressing T-ALL samples on the same array. (C) Heat map of the relative ETV7-expression levels in 50 solid tumor xenografts of the St. Jude expanded panel of pediatric preclinical tumor models using the HG-U133Plus2 GeneChip. Numbers to the right of the heat map represent the relative ETV7 RNA hybridization signals in these xenografts, as determined by the Affymetrix HG-U133Plus2 GeneChip (20). The following tumors were included: BT-36, -41, -44, -54 (ependymoma, p, p, s, s); SK-NEP-1, EW-5, -8, TC-71, CHLA258 (Ewings sarcoma, pr, p, pr, p); GBM2, BT-39, -56, D456, D212, D645 (glioblastoma, p, r, sr, p, s, p); BT-45, -46, -50, -28 (medulloblastoma, p, p, p, p); NB-SD, -1771, -1691, -EBc1, -1643, -1382, CHLA-79, SK-N-AS (neuroblastoma, p, p, p, p, p, p, p, s); OS-1, -2, -17, -29, -31, -33, -9 (osteosarcoma, p, p, p, s, p, p, p); Rh30R, Rh10, Rh28, Rh30, Rh41, Rh65, Rh36 (ARMS, r, p, p, p, p, sr); Rh18, Rh36 (ERMS, p; sr); Bt-29, KT-16, -12, -14 (rhabdoid, p, p, s, p); KT-13, -10, -11, -5 (Wilms tumor, p, p, p, s) (p=primary, s=secondary, pr=primary relapse, sr= secondary relapse, r=relapse). (D) A histogram representing the average ETV7 expression per pediatric tumor type xenograft in the HG-U133Plus2 array as compared with the average ETV7 signal in all tumor xenografts. (E) Histogram of ETV7 expression levels using the Affymetrix U133Av2 array of 46 primary human medulloblastomas (32). The division of ETV7⁺ and ETV7⁻ tumors (relative expression value 200) was based on the hybridization level of ETV7 in non-ETV7-expressing T-ALL samples on the same U133Av2 array.

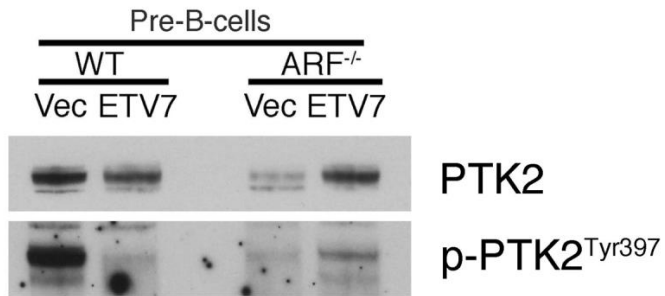
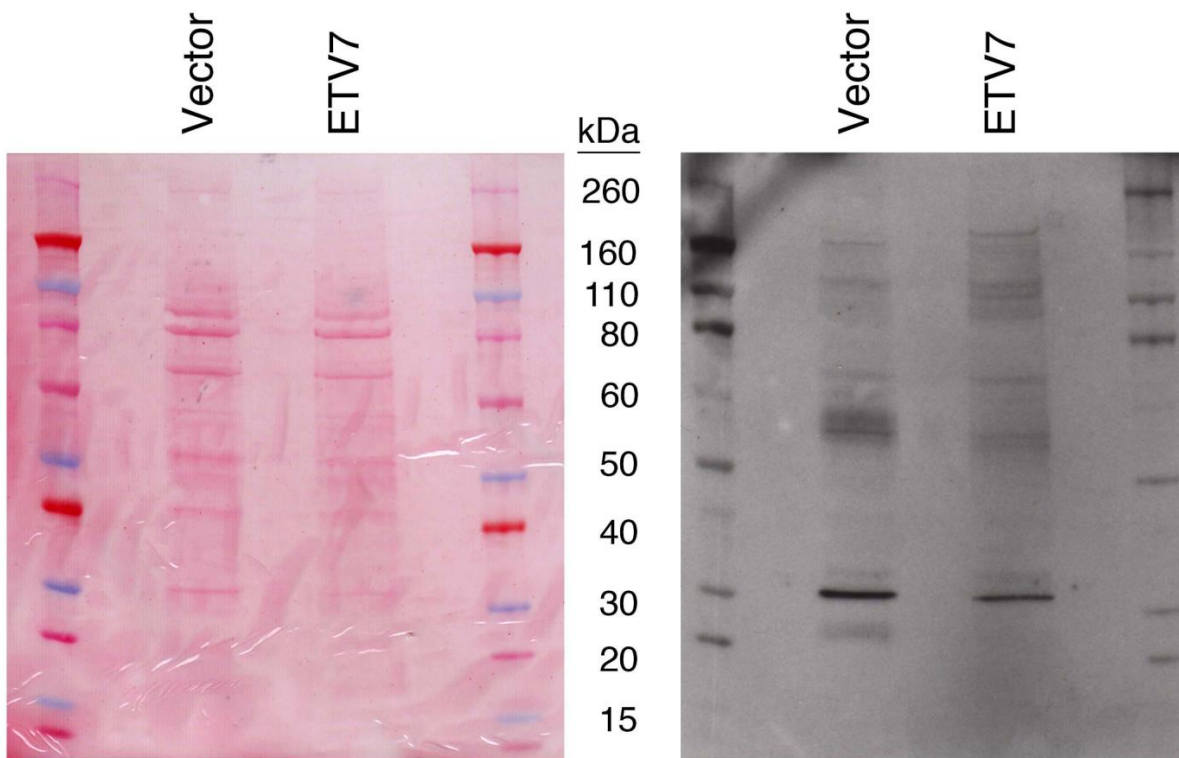
A**B**

Fig. S2. PI3K and PTK2 signaling and anti-p-tyr Western blot of cell lysate of vector and ETV7 mouse pre-B cells. (A) Cell lysates from wild type (WT) and *Arf*^{-/-} mouse pre-B cells (ARF^{-/-}) expressing GFP (Vec) or ETV7 (ETV7) immunoblotted for p-PTK2^{Tyr397} and total PTK2. **(B)** Left panel, Ponceau-S stained nitrocellulose blot of a PAGE gel of lysates of 0.5x10⁶ vector and ETV7 transduced mouse pre-B cells. Right panel, anti-p-tyrosine immunoblot of the same gel.

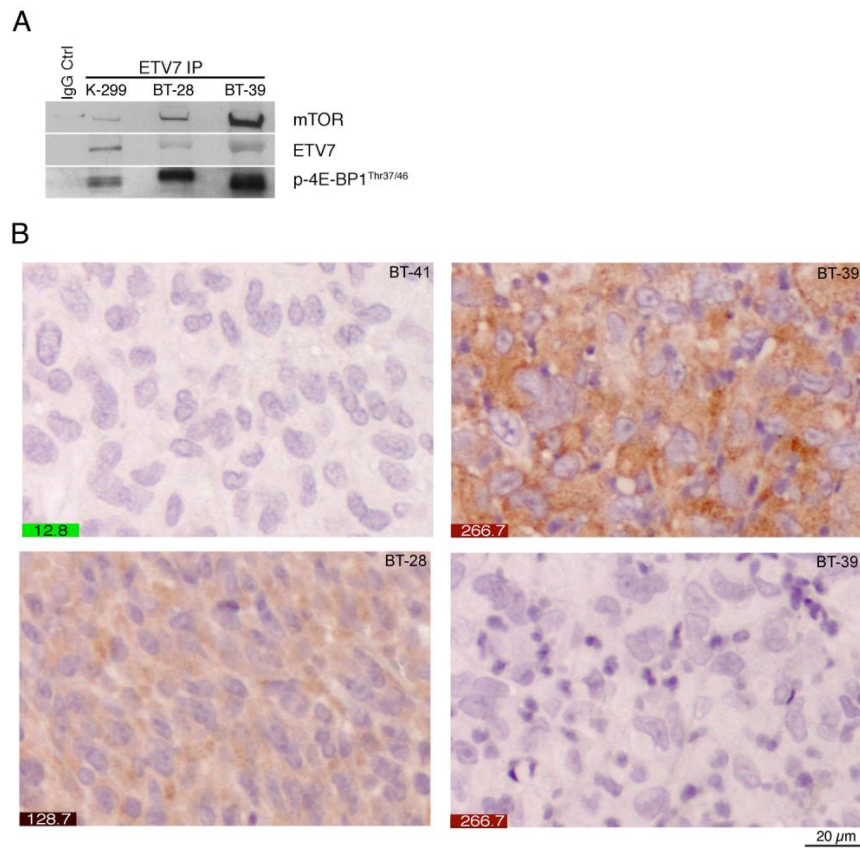
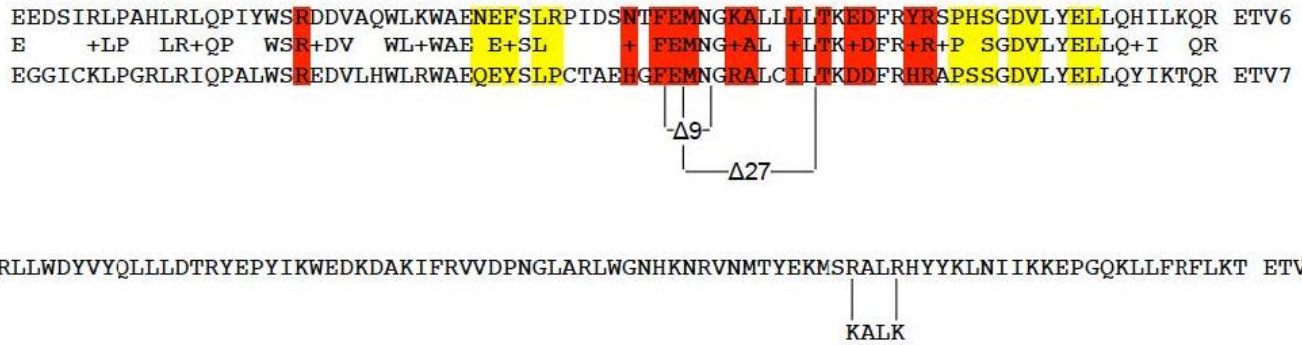


Fig. S3. ETV7 expression in human pediatric tumor xenografts. (A) IPs (ETV7 IP, IgG Ctrl) of lysates from Karpas-299 cells (K-299), and xenograft tumors (BT-28, medulloblastoma; BT-39, glioblastoma) immunoblotted for mTOR, ETV7 or p-4E-BP1^{Thr37/46}. **(B)** ETV7 immunostaining of a BT41 ependymoma xenograft section (no ETV7 expression), a BT28 medulloblastoma xenograft (intermediate ETV7 expression), a BT39 glioblastoma xenograft section (high ETV7 expression) and a BT39 section competed with the peptide against which the anti-ETV7 antibody was raised. Numbers in the lower left corner of the micrographs represent the relative ETV7 RNA hybridization signals in these xenografts, as determined by the Affymetrix HG-U133Plus2 GeneChip, shown in fig. S1C.

A



B

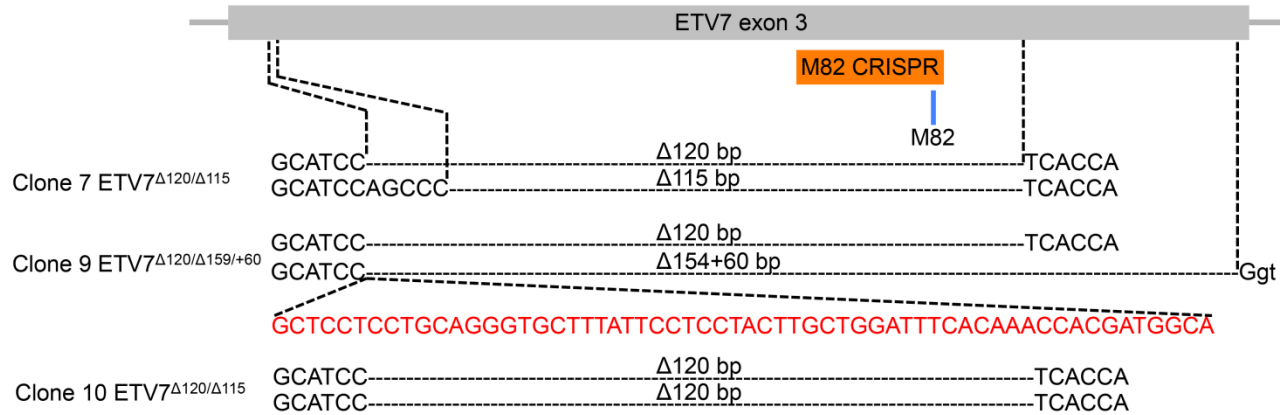


Fig. S4. Sequence comparison of ETV6 and ETV7 PNT domains and the position of $\Delta 9$, $\Delta 27$, $\Delta 120/\Delta 115$, $\Delta 120/\Delta 159/+60$ mutations in the ETV7 PNT domain, and the KALK mutation in the ETV7 ETS domain. (A) The upper part shows the protein sequence comparison of the ETV6 PNT domain (amino acid 44 to 124) with that of the ETV7 PNT domain (amino acid 37 to 117). The line in the middle shows the homology between the two PNT domains. The red and yellow highlights in the ETV6 PNT sequence indicate residues forming the ML and EH interaction surfaces (65), respectively. The sequences in the ETV7 PNT domain coinciding with the ETV6 ML and EH surfaces are also highlighted in red and yellow. $\Delta 9$ ($\Delta E^{81}MN^{83}$) and $\Delta 27$ ($\Delta M^{82}NGRALCIL^{90}$) indicate the ETV7 PNT domain deletion mutants used in Fig. 2E and 2F. The sequence underneath shows the position of the $R^{281}ALR^{284}$ to $K^{281}ALK^{284}$ mutation in the ETV7 ETS domain (amino acids 224 to 307), which prevents DNA binding. (B) Top bar depicts exon 3 of ETV7 (165 bp) with underneath the relative positions of the M82 CRISPR (not to scale) and the methionine 82 codon (M82). Underneath are the partial sequences of Karpas-299-EBNA-Cas9 clones 7, 9 and 10. Clone 9 ($K-E^{\Delta 120/\Delta 159/+60}$) was used for experiments shown in Fig. 5A, 5B, and fig. S7B. Dashed vertical lines demarcate the deletions in the different alleles with the juxtaposed 5' and 3' nucleotide sequences indicated. The 120bp deletion ($\Delta 120$) encodes a highly unstable ETV7 protein with a 40-amino acid (aa) deletion in the PNT domain, including M82, which is undetectable in ETV7 IP/western blots (Fig. 5A, insert). The 115bp deletion encodes an out of frame protein of 63 aa containing the 49 aa ETV7 N-terminus followed by 14 aa from the -1-reading frame. The 154 bp deletion/60 bp insertion (red lettering) encodes a 50-aa protein containing the 49 aa ETV7 N-terminus followed by one non-ETV7 aa.

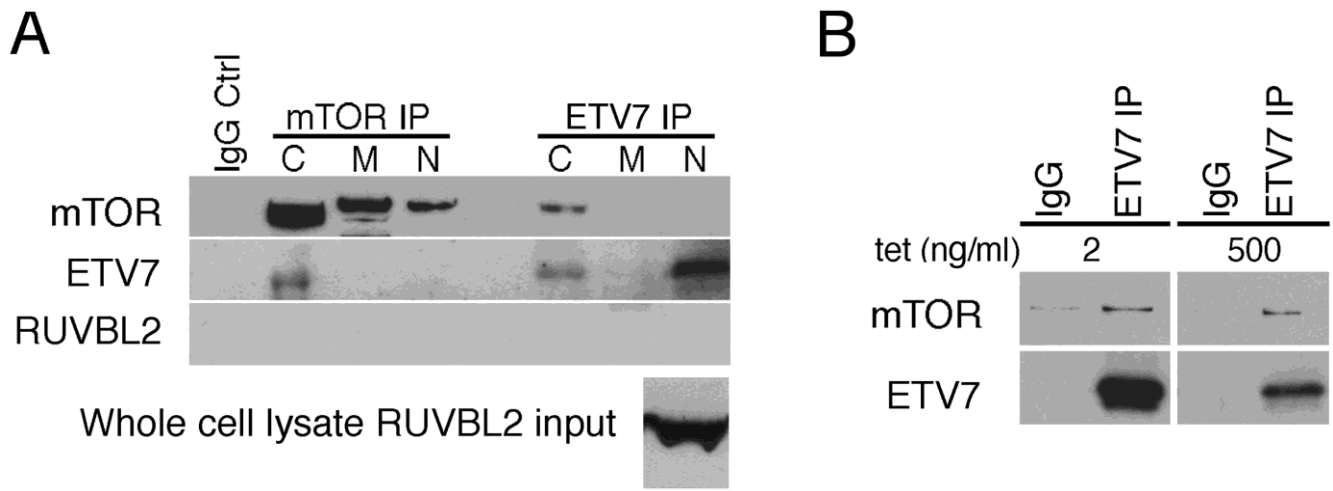


Fig. S5. mTOR localization and assembly. (A) mTOR (mTOR IP) or ETV7 (ETV7 IP) IP of subcellular fractions (C=cytoplasm, M=membrane, N=nucleus) of Karpas-299 cells immunoblotted for mTOR, ETV7 or RUVBL2. (B) IgG or ETV7 IP of lysate from tetracycline-treated (tet) Tet-off U937T cells carrying a tet^{operator}CMV minimal promoter-driven ETV7 construct, immunoblotted for mTOR and ETV7. Higher ETV7 expression (2 ng/mL tetracycline) does not result in more mTOR coprecipitation.

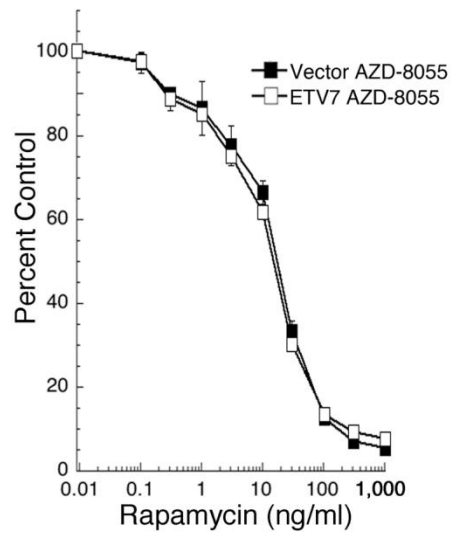
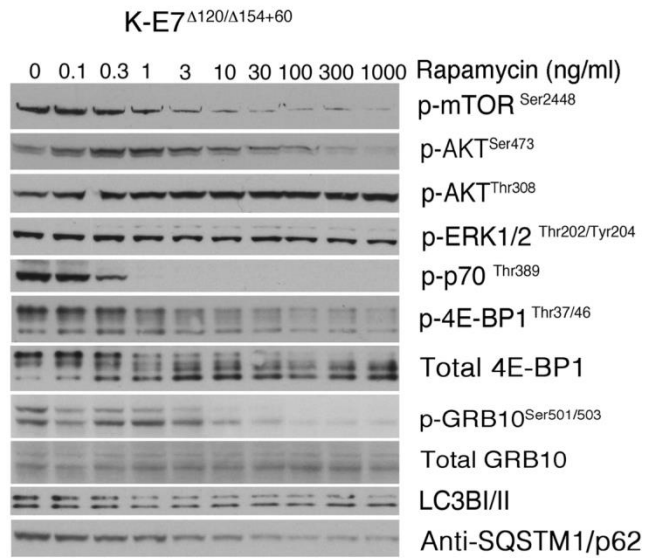
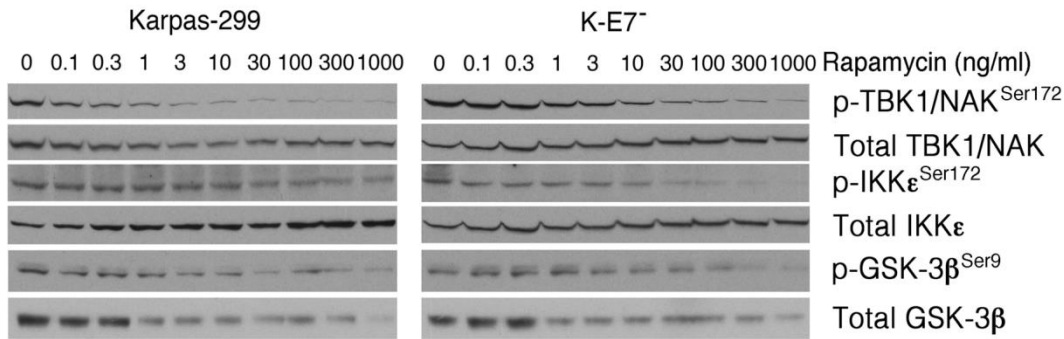
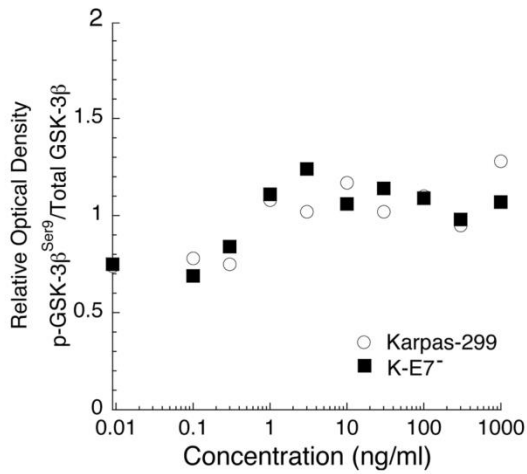
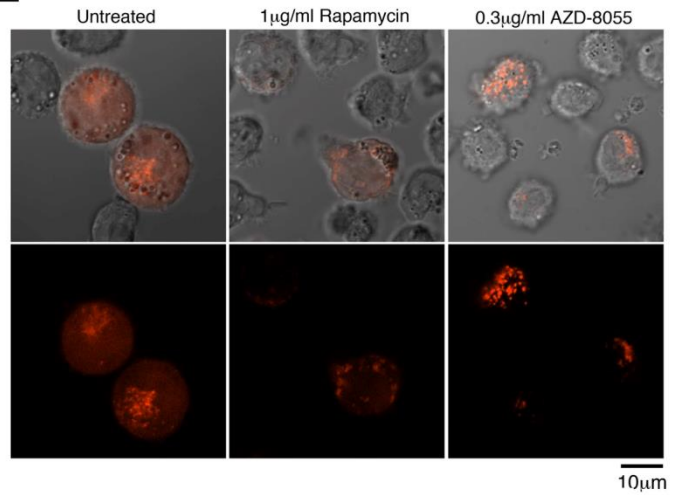
A**B****C****D****E**

Fig. S6. Effects of mTOR inhibitors and mTORC3 loss on mTOR signaling. (A) Proliferating Ew-8 Ewing's sarcoma cells transduced with MSCV-IRES-GFP (vector) or MSCV-ETV7-IRES-GFP (ETV7) were treated with increasing amounts (0.1, 0.3, 1.3, 10, 30, 100, 300, 1,000 ng/mL) of AZD-8055 for 3 population doublings. Cell densities (Percent Control) were plotted as the percentage of cells treated with vehicle. Data are represented as mean +/- SEM from 3 independent experiments. 30% control or less means no proliferation. (B) Immunoblots of K-E7^{Δ120/Δ154+60} cell lysates treated with increasing amounts of rapamycin (0.1, 0.3, 1.3, 10, 30, 100, 300, 1,000 ng/mL) probed for p-mTOR^{Ser2448}, p-AKT^{Ser473}, p-AKT^{Thr308}, p-ERK1/2^{Thr202/Tyr204}, p-p70S6K^{Thr389}, p-4E-BP1^{Thr37/46}, total 4E-BP1, LC3BI/II and SQSTM1/p62. (C) Immunoblots of lysates of equal numbers of Karpas-299, and K-E7' cells were treated with increasing amounts of rapamycin (0.1, 0.3, 1.3, 10, 30, 100, 300, 1,000 ng/mL) and probed for, phospho-IKKε^{Ser172}, total IKKε, phospho-TBK1^{Ser172}, total TBK1, p-GSK3-β^{Ser9} and total GSK3-β. (D) p-GSK3-β^{Ser9} and total GSK3-β band intensities at each rapamycin concentration of the western blot in C were determined using a densitometer and plotted as the p-GSK3-β^{Ser9}/GSK3-β relative intensities to show that loss of p-GSK3-β^{Ser9} signal follows the loss of total GSK3-β. (E) Karpas-299 cells transduced with LC3B-mCherry retrovirus were treated or not (untreated) with rapamycin (1,000ng/ml rapamycin) or AZD-8055 (300 ng/ml AZD-8055) for 72 hours. Cells were visualized using phase contrast/fluorescence microscopy (top row) or fluorescence microscopy alone (bottom row). Only cells treated with AZD-8055 show active autophagy as indicated by punctate staining. mTORC2 signaling in Karpas-299 cells either.

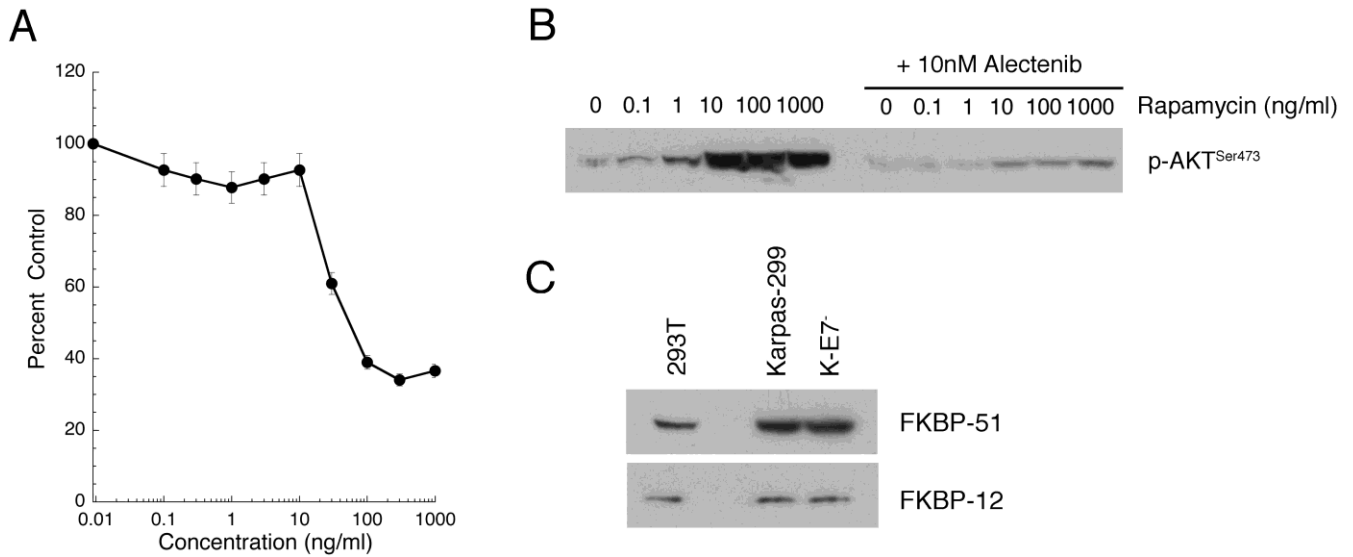


Fig. S7. Effect of ALK inhibition on p-AKT^{Ser473} and relative FK506-binding protein expression in Karpas-299 cells. (A) Proliferating Karpas-299 cells were treated with increasing amounts (0.1, 0.3, 1, 3, 10, 30, 100, 300, 1,000 nM) of the ALK inhibitor alectinib for 3 population doublings. Cell densities (percent control) were plotted as the percentage of cells treated with vehicle. Data are represented as mean +/- SEM from 3 independent experiments. **(B)** Proliferating Karpas-299 cells were treated with increasing amounts (0.1, 1, 10, 100, 1,000 ng/mL) of rapamycin in the absence or presence of 10ng/ml alectinib for 72 hours. Cell lysates were immunoblotted for p-AKT^{Ser473}. Compared to cells treated with rapamycin alone, NPM-ALK inhibition with 10nM alectinib greatly reduced the p-AKT^{Ser473} feedback phosphorylation with increasing rapamycin concentration. **(C)** Lysates of 293T, Karpas-299 and K-E7⁻ cells were immunoblotted for FKBP-12 and FKBP-51. The levels of these two proteins in Karpas-299 and K-E7⁻ cells are similar to that in 293T cells. The relative amounts of FKBP-12 and FKBP-51 in 293T cells are such that they cannot fully inhibit mTORC2 signaling upon long-term rapamycin treatment (40), predicting that they cannot inhibit mTORC2 signaling in Karpas-299 cells either.

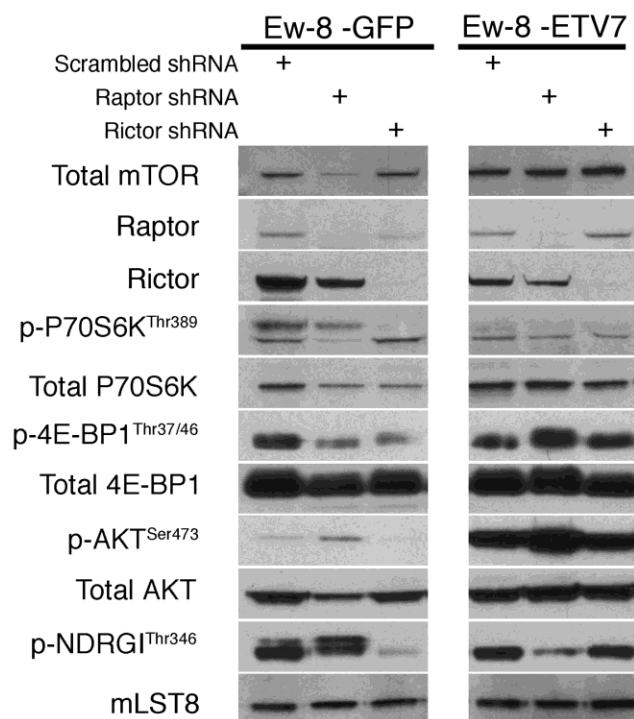
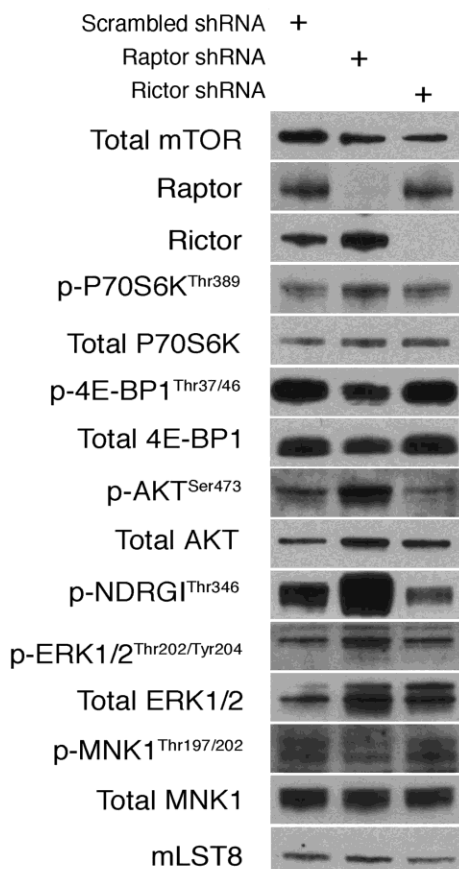
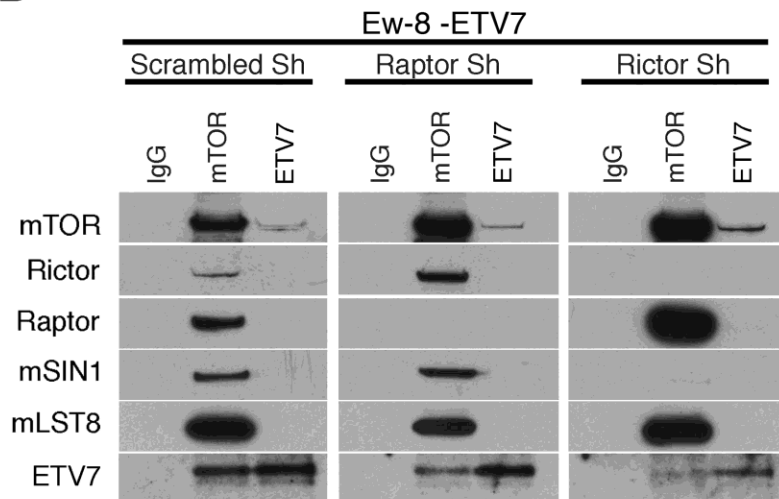
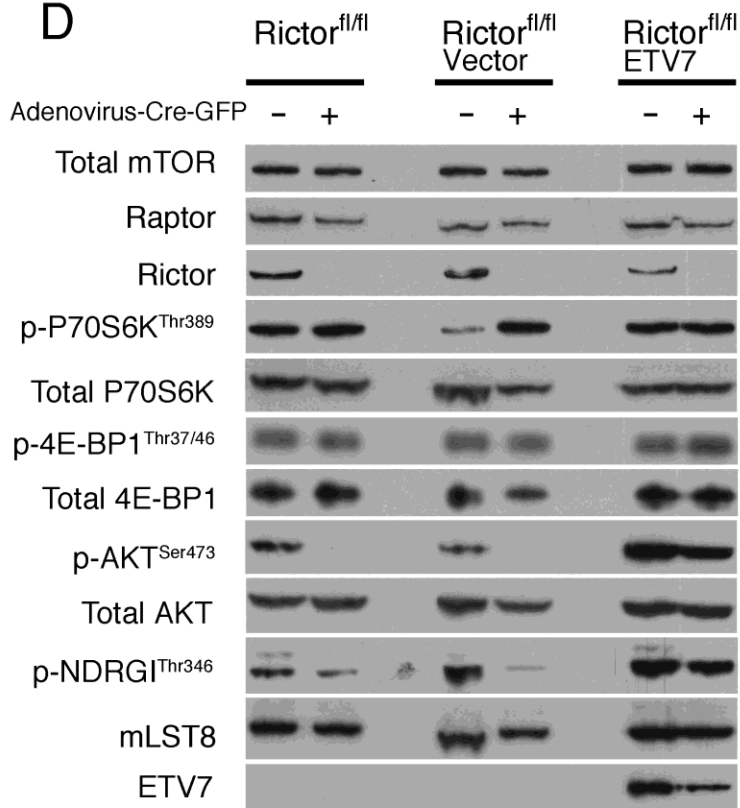
A**C****B****D**

Fig. S8. mTORC3 kinase is insensitive to Raptor or Rictor knockdown or Rictor knockout. (A) Immunoblots of lysates of EW-8 Ewing's sarcoma cells transduced with GFP or ETV7 lentivirus and super transduced with scrambled-shRNA, Raptor-shRNA or Rictor-shRNA lentivirus were probed for mTOR, Raptor, Rictor, p-P70S6K^{Thr389}, total P70S6K, p-4E-BP1^{Thr37/46}, total 4E-BP1, p-AKT^{Ser473}, total AKT, p-NDRG1^{Thr346} and mLST8. **(B)** mTOR and ETV7 IPs of the same EW-8 lysates as in A were immunoblotted for mTOR, Rictor, Raptor, mSIN1, mLST8 and ETV7. **(C)** Lysates of scrambled, Raptor, or Rictor Karpas-299 knockdown cells immunoblotted for mTOR, Rictor, Raptor, p-P70S6K^{Thr389}, total P70S6K, p-AKT^{Ser473}, total AKT, p-NDRG1^{Thr346}, p-4E-BP1^{Thr37/46}, total 4E-BP1, p-ERK1/2^{Thr202/Tyr204}, total ERK1/2, p-MNK1^{Thr197/202}, total MNK1 and mLST8. mLST8 serves as the loading control. **(D)** Ninety hours after infection with Adenovirus-GFP-iCre (+) or not (-), lysates of *Rictor*^{fl/fl} (*Rictor*^{fl/fl}), *Rictor*^{fl/fl}-vector (*Rictor*^{fl/fl}-vector) or *Rictor*^{fl/fl}-ETV7 (*Rictor*^{fl/fl}-ETV7) MEFs were immunoblotted for Rictor, ETV7, p-AKT^{Ser473}, total AKT, p-NDRG1^{Thr346}, Raptor, p-p70S6K^{Thr389}, total p70S6K, p-4E-BP1^{36/47}, total 4E-BP1 and mLST8 as a loading control.

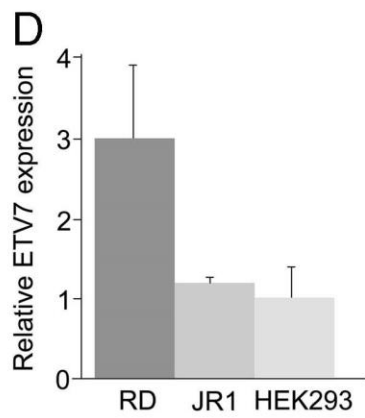
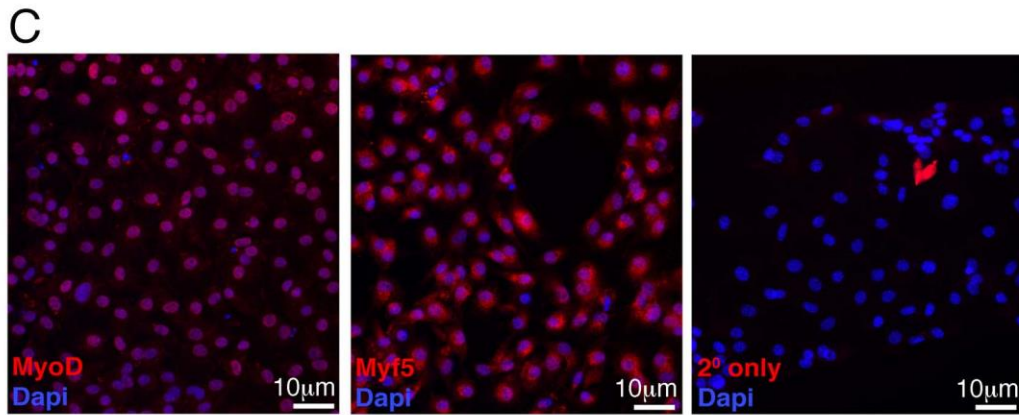
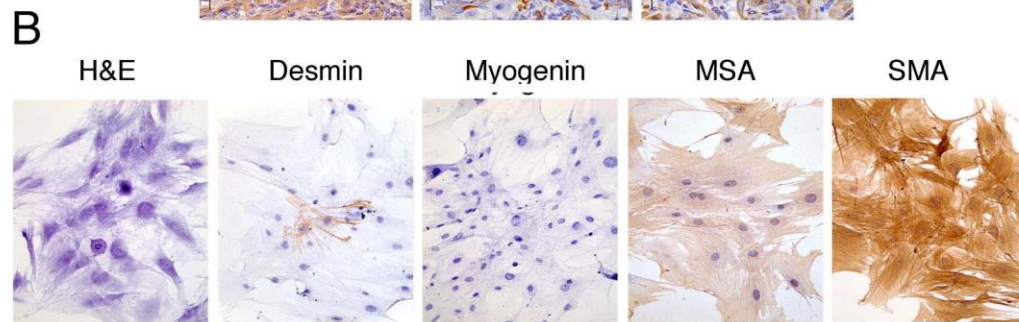
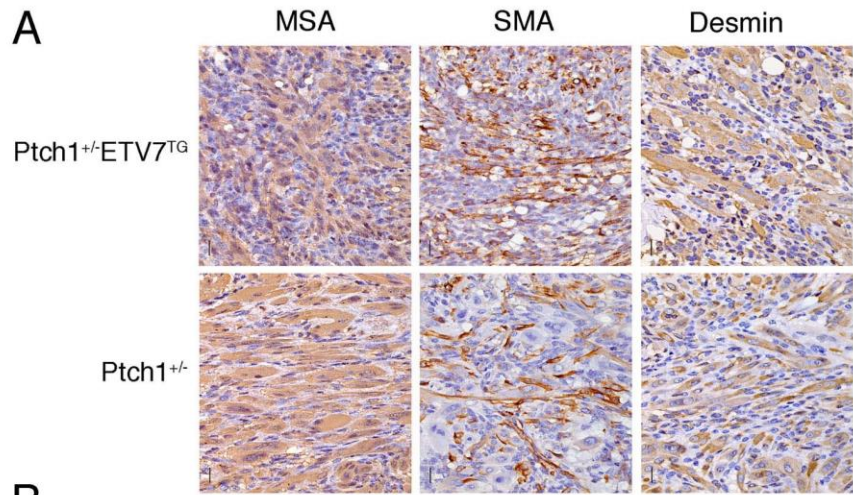


Fig. S9. ERMS-specific markers in $Ptch^{+/-}/ETV^{TG+/-}$ tumors are preserved in $Ptch^{+/-}/ETV^{TG+/-}$ cell lines. (A) Representative example of formalin fixed paraffin embedded sections of a $Ptch1^{+/-}/ETV7^{TG}$ (upper panel) and $Ptch1^{+/-}$ (lower panel) primary tumor stained with MSA antibody, SMA antibody, or desmin antibody. Scale bar represents 20 μ m. (B) Representative example of formalin fixed cell line of a $Ptch1^{+/-}/ETV7^{TG}$ tumor stained with: H&E, anti-Desmin, -Myogenin, -MSA, -SMA antibody. (C) Representative example of formaldehyde fixed cell line of a $Ptch1^{+/-}/ETV7^{TG}$ tumor stained with: MyoD antibody and Dapi, Myf5 antibody and Dapi, Secondary antibody alone and Dapi. Scale bar represents 10 μ m. (D) ETV7 Q-RT-PCR of RNA from ERMS cell lines RD and JR and HEK 293T cells. Q-RT PCR results were normalized to endogenous HPRT expression. Data are the mean +/- SEM from two independent experiments.

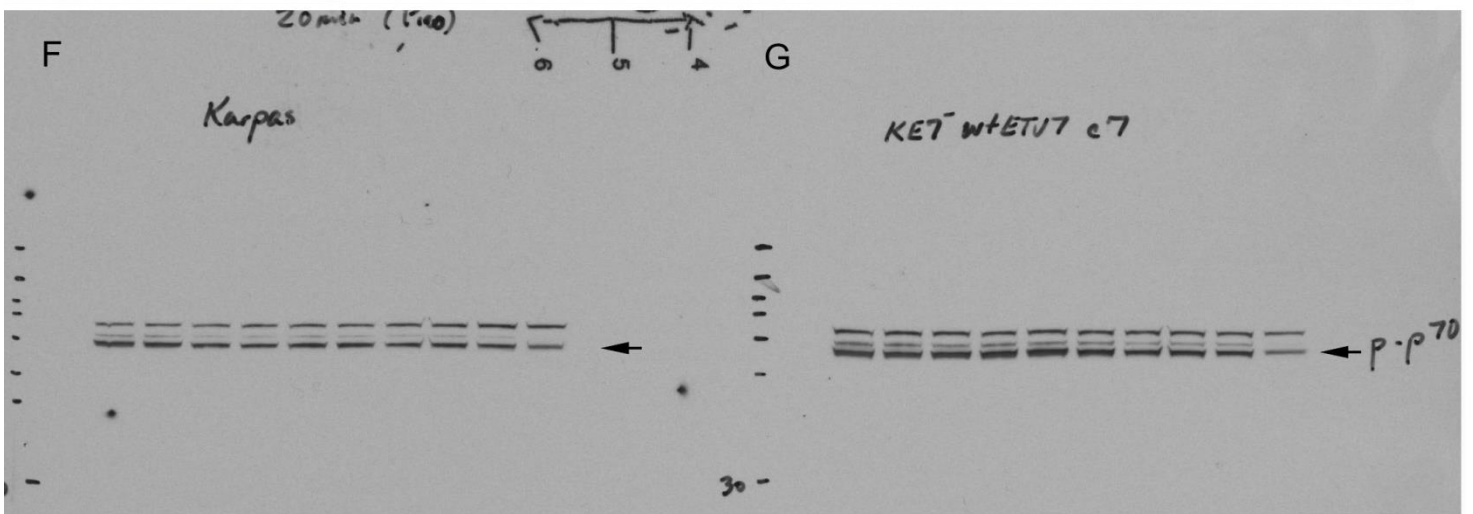
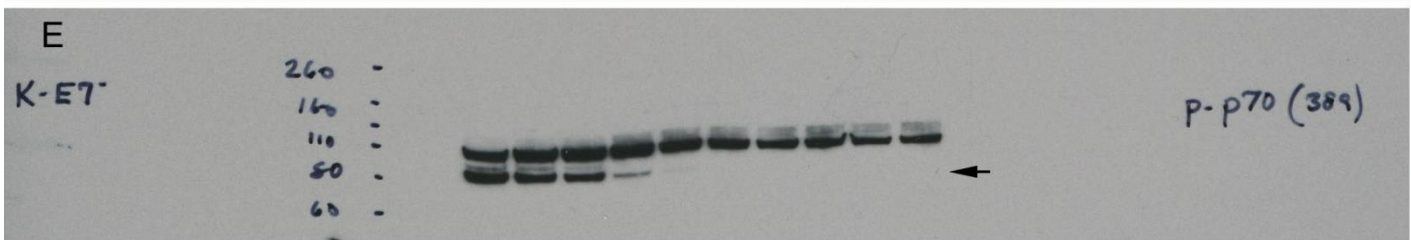
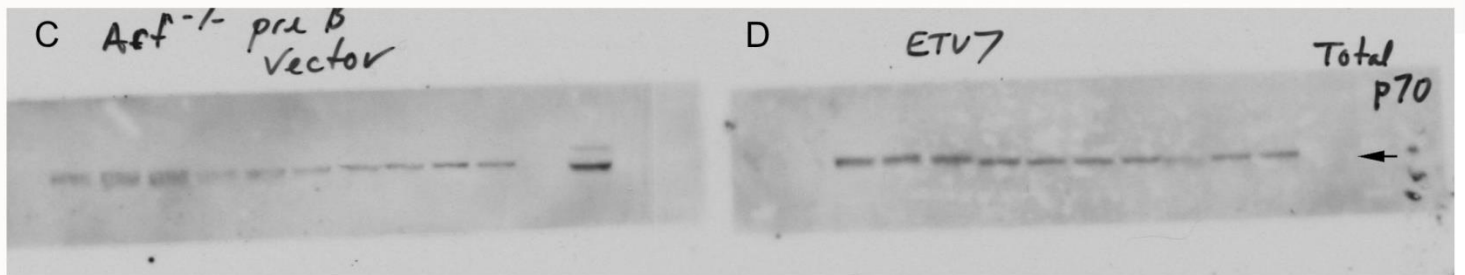
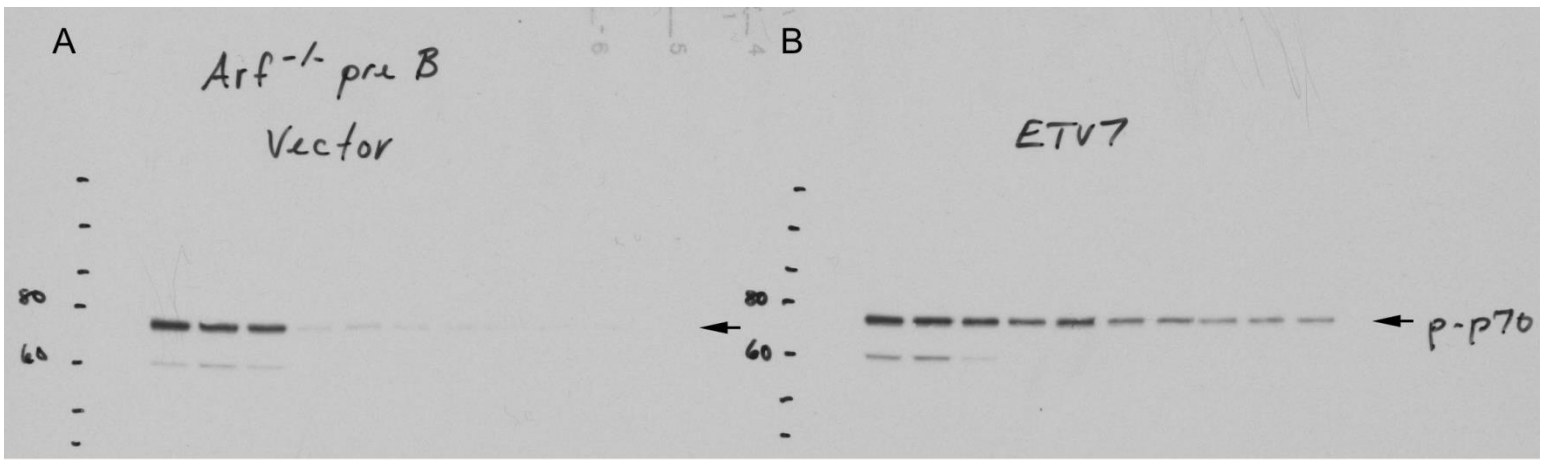


Fig. S10. Whole phospho-p70S6K^{Thr389} and p70S6K Western blots relating to Figs. 1C and 5D. This figure shows images of the whole western blots of lysates of mouse *Arf*^{-/-} pre-B cells expressing (A) vector or (B) ETV7, treated with increasing amounts of rapamycin (from left to right: 0, 0.1, 0.3, 1, 3, 10, 30, 100, 300, 1000 ng/ml rapamycin), probed with the anti-phospho-p70S6K^{Thr389} antibody or the same blots probed with a total anti-p70S6K antibody (C, D). These whole images represent the phospho-p70S6K^{Thr389} and total p70S6K cutouts shown in Fig. 1C. (E, F and G) show KE7 (no ETV7), Karpas-299, and KE7-ETV7 lysates of cells treated with the same increasing amounts of rapamycin, probed with the anti-phospho-p70S6K^{Thr389} antibody. These whole images represent the phospho-p70S6K^{Thr389} cutouts shown in Fig. 5D. The arrows indicate the position of the phospho-p70S6K^{Thr389} or p70S6K bands. The horizontal lines at the left of each blot indicate the position of the molecular weight markers (260, 160, 110, 80, 60, 40, and 30 kDa. respectively).

Table S1. Expression effects of ETV7.**A.** Upregulated ETV7 expression in adult tumor samples.

Tumor Type	Over-expression	Platform
Well Differentiated Liposarcoma (Henderson et al, Genome Biol 6, R76, 2005; Nakayama et al, Modern Pathology, Inc 20,749-59, 2007)	Top 1%	U133A 2.0, U133A
B-cell Acute Lymphoblastic Leukemia (Raetz et al, Pediatric Blood Cancer 47, 130-40, 2006).	Top 1%	U133A
Esophageal Carcinoma (Kimchi et al, Cancer Research 65, 3146-54, 2005)	Top 1%	U133A
Invasive Ductal Breast Carcinoma (Turashvili et al, BMC Cancer 7, 55, 2007)	Top 1%	U133 Plus 2.0
Liver Cell Dysplasia vs. Normal (Wurmbach, Hepatology 45, 938-47, 2007)	Top 1%	U133 Plus 2.0
B-cell Acute Lymphoblastic Leukemia (Maia et al, Cancer Res 65, 10050-58, 2005; Bhojwani et al, Blood 108, 711-17, 2006)	Top 5%	U133A
Superficial Bladder Cancer (Modlich et al, Clin Cancer Res 10, 3410-21, 2004)	Top 5%	U133A
Gastric mixed Adenocarcinoma (Ooi et al, PLoS Genet 5, e1000676, 2010)	Top 5%	U133A
Pleomorphic Myxofibrosarcoma vs. Normal (Barretina et al, Nat Genet 42, 715-21, 2010)	Top 5%	U133A
Ovarian Clear Cell Adenocarcinoma (Lu et al, Clin Cancer Res 10, 3291-00, 2004)	Top 5%	U95D
Ductal breast carcinoma (Turashvili et al, BMC Cancer 7, 55, 2007)	Top 5%	U133 Plus 2.0
Gastric Cancer (Bittner et al, GCEPO, 2005)	Top 5%	U133 Plus 2.0
Liver Cirrhosis vs. Normal (Wurmbach, Hepatology 45, 938-47, 2007)	Top 5%	U133 Plus 2.0
Acute Myeloid Leukemia FAB subtype M5 (Metzeler et al, Blood 112, 4193-01, 2008)	Top 5%	U133 Plus 2.0
Gastric Intestinal Type Adenocarcinoma (Ooi et al, PLoS Genet 5, e1000676 2010)	Top 5%	U133 Plus 2.0
Gastrointestinal Part: Descending Colon (Sabates-Bellver et al, Mol Cancer Res 5, 1263-75, 2007)	Top 5%	U133 Plus 2.0
Renal Carcinoma (Yusenko et al, BMC Cancer 9, 152, 2009)	Top 5%	U133 Plus 2.0
Leukemia Precursor (Wouters et al, Blood 113, 3088-91, 2009)	Top 5%	U133 Plus 2.0
Clear Cell Renal Cell Carcinoma (Bittner et al, GCEPO, 2005, Yusenko et al, BMC Cancer 9, 152, 2009)	Top 5%	U133 Plus 2.0
Brain Part: Brain Nucleus (Su et al, Proc Natl Acad Sci USA, 101, 6062-67, 2004)	Top 10%	U133A
Malignant Fibrous Histiocytoma (Detwiler et al, Cancer Res 65, 5881-89, 2005)	Top 10%	U133A
Ovarian Clear Cell Carcinoma vs. Normal (Hendrix et al, Cancer Res 66, 1354-62, 2006)	Top 10%	U133A
Invasive Ductal Breast Carcinoma (Radvanyi et al, Proc Natl Acad Sci USA, 102, 11005-10, 2005)	Top 10%	Hu03 Custom

Brain Part: Putamen (Roth et al, Neurogenetics 7, 67-80, 2006)	Top 10%	U133 Plus 2.0
Ductal Breast Carcinoma (Kimchi et al, Cancer Research 65, 3146-54, 2005, Roth et al, Neurogenetics 7, 67-80, 2006, Richardson et al, Cancer Cell 9, 121-32, 2006)	Top 10%	U133 Plus 2.0
Medullary Breast Cancer (Ginestier et al, Clin Cancer Res 12, 4533-44, 2006)	Top 10%	U133 Plus 2.0
Bladder Cancer (Bittner et al, GCEPO, 2005)	Top 10%	U133 Plus 2.0
Cecum Adenocarcinoma (Kaiser et al, Genome Biol 8, R131, 2007)	Top 10%	U133 Plus 2.0
Germinal Center B-Cell-Like Diffuse Large B-cell Lymphoma (Lentz et al, N Eng J Med 359, 2313-23, 2006)	Top 10%	U133 Plus 2.0
Type 3 Diffuse Large B-Cell Lymphoma (Lentz et al, N Eng J Med 359, 2313-23, 2006)	Top 10%	U133 Plus 2.0
Type II Endometrial Carcinoma (Bittner et al, GCEPO, 2005)	Top 10%	U133 Plus 2.0
Liver Cirrhosis vs. Normal (Wurmbach, Hepatology 45, 938-47, 2007)	Top 10%	U133 Plus 2.0
Acute Myeloid Leukemia FAB subtype M5 (Kool et al, PLoS One 3, e3088, 2008)	Top 10%	U133 Plus 2.0

B: Differential expression (log2 ratio) of mTOR-related genes in vector versus ETV7 ARF^{-/-} mouse pre-B cells as determined by Affymetrix array analysis.

C: Differential expression (log2 ratio>0.5) of kinase genes in vector versus ETV7 ARF^{-/-} mouse pre-B cells as determined by Affymetrix array analysis.

D: Differential expression (log2 ratio>0.5) of cytokine, growth factor and growth factor receptor genes in vector versus ETV7 ARF^{-/-} mouse pre-B cells as determined by Affymetrix array analysis.

B		C		D	
Gene Symbol	ETV7 vs Vector	Gene Symbol	ETV7 vs Vector	Gene Symbol	ETV7 vs Vector
Prkaa2	0.90428	Ptk2	1.61	Gpr12	1.37
Grb10	0.56929	Irak3	0.97	Ccl9	1.37
Deptor	0.3964	Prkaa2	0.90	Olfr820	1.04
Prkar2b	0.32123	Camk4	0.80	Il12rb2	0.97
Mtor	0.2073	Ak4	0.80	Trav9d-1	0.90
Lamtor3	0.20379	Cdk14	0.73	Trav9d-4	0.89
Lamtor5	0.2028	Mapk11	0.71	Trav16n	0.88
Lamtor3	0.1998	Plk2	0.62	Mc1r	0.82
Prkab2	0.18871	Rps6kl1	0.59	Igf2r	0.67
Lamtor1	0.16293	Pfkfb	0.56	Lrp4	0.67
Prkab1	0.1521	Nim1k	0.56	Ccl6	0.66
Prkag1	0.1283	Lck	0.53	Vmn2r51	0.64
Prkar1b	0.1213	Pkmyt1	0.53	Gpr125	0.64
Lamtor2	0.10599	Tnk2	0.51	Bmpr1a	0.64
Mlst8	0.05355	Itpkb	-0.51	Bmp4	0.64
Prkar1a	0.04963	Camk1d	-0.52	Trav9-2	0.61
Pten	-0.0131	Pik3r3	-0.52	Trav6-3	0.61
Prkag3	-0.02545	Ak5	-0.54	Tnfrsf22	0.58
Prkaa1	-0.0395	Sik1	-0.56	Tnfrsf22	0.58
Tsc2	-0.04166	Ret	-0.56	Olfr1437	0.56
Prkacb	-0.0426	Eif2ak2	-0.57	Olfr1238	0.56
Rptor	-0.09697	Pik3cg	-0.59	Olfr687	0.53
Rictor	-0.09717	Map3k8	-0.61	Nr1d1	0.53
Prkag2	-0.10246	Pik3r5	-0.62	Tnk2	0.51
Tsc1	-0.10304	Ryk	-0.69	Fcgr3	0.51
Lamtor4	-0.24397	Bmpr2	-0.71	Ifnab	0.51
Prkaca	-0.25174	Prkccq	-0.84	Olfr988	0.50
Prkar2a	-0.43749	Dgka	-1.04	Olfr205	-0.52
		Hck	-1.09	Igf1r	-0.52
		Adck1	-1.12	Tgfbr2	-0.52
				Tgfbr3	-0.52
				Angptl2	-0.52
				Tnf	-0.52
				Fcrla	-0.53
				Lpar6	-0.53
				Cysltr1	-0.54
				Il4ra	-0.54
				Klrb1a	-0.55
				Milr1	-0.56
				Csf2rb	-0.56
				Vmn2r41	-0.60
				Olfr1205	-0.61
				Chrn1	-0.63
				Igf2bp3	-0.64
				Gria2	-0.68
				Ryk	-0.69
				Gpr84	-0.71
				Il5ra	-0.71
				Olfr372	-0.72
				Tnfrsf13c	-0.72
				Igf1bp4	-0.72
				Gprc5b	-0.76
				Fcrl6	-0.77
				Nr2c1	-0.81
				Ephb2	-0.83
				Gpr174	-0.87
				Gpr128	-0.90
				Tlr9	-0.96
				Klrb1f	-0.97
				Il2ra	-0.99
				Tnfsf8	-0.99
				Bmpr2	-1.10
				P2ry13	-1.10
				Igf1	-1.13
				Sorl1	-1.33
				Csf2rb2	-1.40
				Gpr18	-1.41
				Il18	-1.42
				Il10ra	-1.46
				Igf2	-1.97

E: Gene Set Enrichment Analysis using Hallmark and canonical databases identifying ETV7 up and down regulated pathways in ETV7 versus vector ARF^{-/-} mouse pre-B cells.

E

Up regulated Hallmark pathways

NAME	SIZE	NES	NOM p-val	FDR q-val
HALLMARK_MYC_TARGETS_V2	57	1.849533	0	0.005558
HALLMARK_MYC_TARGETS_V1	195	1.839917	0	0.00335
HALLMARK_E2F_TARGETS	194	1.807984	0	0.002945
HALLMARK_MTORC1_SIGNALING	189	1.737239	0	0.007111
HALLMARK_APICAL_SURFACE	44	1.632676	0.010504	0.014033
HALLMARK_HEDGEHOG_SIGNALING	36	1.543138	0.025341	0.027647
HALLMARK_FATTY_ACID_METABOLISM	145	1.505772	0.004695	0.035686
HALLMARK_OXIDATIVE_PHOSPHORYLATION	190	1.504944	0.002217	0.031484
HALLMARK_SPERMATOGENESIS	132	1.497038	0.00432	0.030267
HALLMARK_ANGIOGENESIS	35	1.419507	0.057971	0.053691
HALLMARK_CHOLESTEROL_HOMEOSTASIS	68	1.399752	0.044118	0.058805
HALLMARK_UNFOLDED_PROTEIN_RESPONSE	111	1.286486	0.069869	0.132809
HALLMARK_GLYCOLYSIS	191	1.164008	0.141256	0.306158
HALLMARK_ADIPOGENESIS	194	1.161185	0.143498	0.289727
HALLMARK_G2M_CHECKPOINT	193	1.033894	0.366667	0.598651
HALLMARK_XENOBIOTIC_METABOLISM	187	1.029852	0.375556	0.574139
HALLMARK_BILE_ACID_METABOLISM	110	0.971861	0.519427	0.727518
HALLMARK_PEROXISOME	99	0.929117	0.636364	0.826374
HALLMARK_PI3K_AKT_MTOR_SIGNALING	104	0.893945	0.703872	0.898499
HALLMARK_DNA_REPAIR	136	0.884729	0.745614	0.88112
HALLMARK_MYOGENESIS	197	0.859496	0.842105	0.903522
HALLMARK_HEME_METABOLISM	179	0.784741	0.96083	0.999151
HALLMARK_WNT_BETA_CATENIN_SIGNALING	41	0.772495	0.836032	0.970219
HALLMARK_PROTEIN_SECRETION	94	0.768796	0.909457	0.933819

Down regulated Hallmark pathways

NAME	SIZE	NES	NOM p-val	FDR q-val
HALLMARK_INTERFERON_ALPHA_RESPONSE	86	-2.31227	0	0
HALLMARK_INTERFERON_GAMMA_RESPONSE	183	-2.22526	0	0
HALLMARK_INFLAMMATORY_RESPONSE	194	-1.70631	0.001739	0.014258
HALLMARK_TNFA_SIGNALING_VIA_NFKB	195	-1.68275	0	0.013594
HALLMARK_ALLOGRAFT_REJECTION	182	-1.51006	0.005386	0.062058
HALLMARK_IL6_JAK_STAT3_SIGNALING	85	-1.4678	0.016227	0.07681
HALLMARK_UV_RESPONSE_DN	142	-1.34444	0.037801	0.177414
HALLMARK_APOPTOSIS	156	-1.34156	0.044405	0.159596
HALLMARK_COMPLEMENT	181	-1.33302	0.031308	0.151301
HALLMARK_TGF_BETA_SIGNALING	54	-1.3122	0.109959	0.162122
HALLMARK_ANDROGEN_RESPONSE	94	-1.30829	0.078755	0.151324
HALLMARK_EPITHELIAL_MESENCHYMAL_TRANSITION	194	-1.28012	0.063636	0.17192
HALLMARK_KRAS_SIGNALING_UP	190	-1.23218	0.082437	0.226756
HALLMARK_COAGULATION	130	-1.20748	0.13594	0.24977
HALLMARK_REACTIVE_OXIGEN_SPECIES_PATHWAY	44	-1.18368	0.215606	0.272473
HALLMARK_IL2_STAT5_SIGNALING	194	-1.13565	0.186257	0.347795
HALLMARK_NOTCH_SIGNALING	31	-1.0307	0.380567	0.59108
HALLMARK_ESTROGEN_RESPONSE_EARLY	197	-1.0261	0.375235	0.571045
HALLMARK_HYPOXIA	192	-0.94878	0.591228	0.770025
HALLMARK_P53_PATHWAY	195	-0.93745	0.589161	0.764326
HALLMARK_UV_RESPONSE_UP	145	-0.91001	0.625229	0.803595
HALLMARK_KRAS_SIGNALING_DN	189	-0.89046	0.747715	0.8224
HALLMARK_PANCREAS_BETA_CELLS	39	-0.8738	0.67086	0.830947
HALLMARK_ESTROGEN_RESPONSE_LATE	191	-0.86581	0.777972	0.816015
HALLMARK_MITOTIC_SPINDLE	195	-0.84197	0.853933	0.838576
HALLMARK_APICAL_JUNCTION	194	-0.76891	0.960303	0.923438

F continued

Transcript ID	Gene Symbol	KALK vs ETV7	Transcript ID	Gene Symbol	KALK vs ETV7
16784098	FRMD6	-0.57	16961094	---	-0.77
17092817	---	-0.57	16929396	---	-0.77
16908817	---	-0.57	17095150	TLE1	-0.78
16772583	---	-0.57	16858118	SNORD105	-0.78
16926754	S100B	-0.57	17078751	REXO1L1P	-0.79
16722890	ANO5	-0.58	16995848	SEPP1	-0.79
17078558	PAG1	-0.58	16760889	C3AR1	-0.79
16685330	GRIK3	-0.58	17104253	MSN	-0.79
16835592	NGFR	-0.58	16680258	MXRA8	-0.79
16877667	FKBP1B	-0.58	17116344	XKRY2	-0.80
17116497	---	-0.59	17117044	XKRY2	-0.80
17099701	MIR3689D2	-0.59	17010175	OGFRL1	-0.80
17093083	---	-0.59	16934300	---	-0.80
16870200	BST2	-0.59	16879250	GALM	-0.81
16845518	TMEM101	-0.59	16853855	---	-0.83
16885842	GPR39	-0.59	16979163	ARSJ	-0.84
16959805	RBP1	-0.59	16681924	PRAMEF14	-0.84
16833476	DHRS11	-0.59	16762154	ABCC9	-0.85
16844356	TNS4	-0.60	17004198	FOXF2	-0.85
17093059	---	-0.60	16677254	SNORA16B	-0.86
16918663	MMP24-AS1	-0.60	16917183	JAG1	-0.86
17019935	PKHD1	-0.60	16850428	ROCK1P1	-0.87
16997141	---	-0.60	16887900	---	-0.88
16948136	---	-0.60	16882821	---	-0.88
16945187	---	-0.60	16770664	TBX5	-0.89
16748529	GPRC5A	-0.60	17116028	TBL1Y	-0.90
16913486	VSTM2L	-0.60	17092794	HACD4	-0.90
16947873	---	-0.60	16873174	ZNF229	-0.91
16947018	---	-0.60	16833426	CCL4L2	-0.91
16698980	SLC30A1	-0.60	16774405	DNAJC15	-0.92
16752870	INHBC	-0.60	16860123	ZNF486	-0.92
17116894	FAM197Y9	-0.60	17110920	PAGE1	-0.92
16819207	MT2A	-0.60	16833420	CCL4	-0.93
17055447	MEOX2	-0.60	16870776	ZNF826P	-0.93
16995914	CCL28	-0.60	16788657	SNORD114-11	-0.95
16981791	---	-0.60	16691090	PTPN22	-0.96
16726880	NEAT1	-0.61	16735938	LINC00958	-0.98
16777882	LOC105370145	-0.61	16870782	ZNF737	-0.98
16866081	ZIK1	-0.61	16819264	MT1X	-0.98
17094191	---	-0.61	16924878	TIAM1	-0.99
17117829	LOC105372488	-0.61	16919242	MAFB	-1.00
16676167	PRELP	-0.62	16979825	PABPC4L	-1.00
16912900	ASIP	-0.62	17058863	CCL26	-1.01
16906175	FRZB	-0.62	16709405	PLEKHS1	-1.02
17077723	CYP7B1	-0.62	16855906	NETO1	-1.03
16788616	SNORD114-1	-0.62	16854660	---	-1.03
17070094	---	-0.62	16748590	EMP1	-1.04
17085073	---	-0.62	16719638	LOC102725247	-1.04
17004208	FOXC1	-0.63	17057868	LINC01446	-1.05
16691016	LINC01356	-0.63	16838017	GALR2	-1.06
16757090	---	-0.63	16829505	---	-1.07
16788683	SNORD114-21	-0.63	17094358	---	-1.09
16931514	---	-0.63	17092268	GLDC	-1.09
16746217	---	-0.63	16816018	MIR365A	-1.10
17048879	ARPC1B	-0.63	16998551	SLCO4C1	-1.11
17096457	CORO2A	-0.63	16753914	LYZ	-1.13
16850892	---	-0.64	17099703	MIR3689E	-1.13
17024079	MAP3K5	-0.64	16870984	ZNF681	-1.18
16982699	SLC6A19	-0.64	16657746	---	-1.20
17079407	TSPYL5	-0.64	17024305	---	-1.23
16862491	TMEM91	-0.64	17018615	ETV7	-1.24
17100655	---	-0.65	17046407	ZNF727	-1.24
16915564	---	-0.65	16862563	CEACAM6	-1.28
16744104	---	-0.65	16941230	GRM2	-1.28
16947148	ARHGEF26	-0.65	17046817	WBSCR17	-1.30
17099699	MIR3689B	-0.65	16716782	PDLIM1	-1.30
17099695	MIR3689A	-0.65	16698234	FMOD	-1.31
16683624	RUNX3	-0.65	16966240	CHRNA9	-1.32
16767324	SNORA70G	-0.65	17107867	MAGEA6	-1.36
16853325	HSBP1L1	-0.65	16754118	LOC105369827	-1.41
16846532	DLX3	-0.65	17097211	PTGR1	-1.44
16788691	SNORD114-25	-0.65	16783729	LOC644919	-1.61
16951557	---	-0.65	16691755	---	-1.61
16853472	---	-0.66	16944618	CD86	-1.62
16782010	TRAJ59	-0.66	16911432	SLX4IP	-1.66
16817624	SPN	-0.66	16781897	TRAV8-6	-1.67
17087133	---	-0.66	16942958	EPHA3	-1.72
16885502	RAB6C	-0.66	16713395	---	-1.77
16942560	ARL6IP5	-0.67	16990267	PCDHB5	-1.98
16762992	LOC105369724	-0.67	16885244	CNTNAP5	-2.13
16737422	---	-0.67	16659371	PRAMEF1	-2.13
16780640	LOC105370333	-0.68	17020497	---	-2.15
16835556	ABI3	-0.69	16681907	PRAMEF14	-2.19
16840318	NLRP1	-0.69	17116675	---	-2.26
16972987	---	-0.70	17114520	ARHGEF6	-2.97
17044193	LOC101927841	-0.70	16736773	SLC5A12	-3.83
17077267	---	-0.70	16977052	CXCL10	-3.84
16834196	FKBP10	-0.70	---	---	---
16967273	---	-0.70	---	---	---
16670164	---	-0.71	---	---	---
17059119	SEMA3C	-0.71	---	---	---
16973934	CYTL1	-0.71	---	---	---
16900189	---	-0.72	---	---	---
17090296	ASS1	-0.72	---	---	---
16718252	LOC102724418	-0.72	---	---	---
16695508	TSTD1	-0.73	---	---	---
16912362	ID1	-0.73	---	---	---
17019543	LOC101929705	-0.73	---	---	---
17070482	---	-0.73	---	---	---
17020787	MB21D1	-0.74	---	---	---
17005858	HIST1H2AI	-0.74	---	---	---
16965606	SLC34A2	-0.74	---	---	---
16971272	EDNRA	-0.75	---	---	---
16957263	DPPA4	-0.75	---	---	---
16815310	TNFRSF12A	-0.75	---	---	---
16778829	CPB2	-0.75	---	---	---
16704237	---	-0.76	---	---	---
16983159	---	-0.76	---	---	---
17002874	---	-0.76	---	---	---
17048742	NPTX2	-0.76	---	---	---

G: Mass spectrometry analysis of purified Origene human ETV7 protein.

H: Mass spectrometry analysis of purified Origene human mTOR protein.

G

H

Description	Spectral Count	Total Peptides	Description	Spectral Count	Total Peptides
Transcription factor ETV7	716	20	Serine/threonine-protein kinase mTOR	1341	187
Tubulin beta chain	29	12	Heat shock 70 kDa protein 1A/1B	215	38
Tubulin beta-4A chain	29	11	Heat shock cognate 71 kDa protein	162	34
Heat shock 70 kDa protein 1A/1B	21	12	Heat shock 70 kDa protein 1-like	104	13
Tubulin beta-2A chain	20	8	Protein arginine N-methyltransferase 5	85	26
Pyruvate kinase PKM	17	11	Heat shock cognate 71 kDa protein (Fragment)	80	12
Heat shock protein HSP 90-beta	14	11	Tubulin beta-4B chain	61	18
L-lactate dehydrogenase B chain	14	7	Tubulin beta chain	56	16
Elongation factor 2	14	7	Tubulin beta-4A chain	49	14
Heat shock cognate 71 kDa protein	11	8	Heat shock 70 kDa protein 6	46	8
Histone H2B type 1-O	11	2	Kinesin-like protein KIF11	44	25
Histone H2B type 1-H	11	2	Tubulin beta-2A chain	42	12
Heat shock 70 kDa protein 6	10	5	Tubulin beta-2B chain	42	12
Histone H4	9	4	Methylosome protein 50	42	11
Guanine nucleotide-binding protein subunit beta-2-like 1	9	7	Protein phosphatase 1B	41	18
Heat shock protein HSP 90-alpha	7	5	Heat shock 70 kDa protein 4	38	23
Heat shock cognate 71 kDa protein (Fragment)	6	4	60 kDa heat shock protein, mitochondrial	36	23
ATP-dependent RNA helicase A	6	6	Stress-70 protein, mitochondrial	33	17
Actin, gamma-enteric smooth muscle	5	1	Tubulin beta-3 chain	26	7
ATP synthase subunit beta, mitochondrial	5	5	Heat shock protein 105 kDa	23	18
Glyceraldehyde-3-phosphate dehydrogenase	4	3	BAG family molecular chaperone regulator 2	18	10
40S ribosomal protein S14	4	2	Ubiquitin (Fragment)	16	4
Rab GDP dissociation inhibitor alpha	4	3	Tubulin beta-8 chain	14	4
ATP synthase subunit alpha, mitochondrial	4	4	40S ribosomal protein S3	11	9
Histone H2A type 1-D	4	2	ADP/ATP translocase 2	11	7
Histone H1.2	4	3	Heat shock protein HSP 90-beta	9	9
Elongation factor 1-alpha 1	4	3	78 kDa glucose-regulated protein	9	4
Ubiquitin (Fragment)	4	2	Ubiquitin-40S ribosomal protein S27a	9	3
Nuclease-sensitive element-binding protein 1	4	4	Heat shock 70 kDa protein 4L	9	9
L-lactate dehydrogenase A chain 2	4	3	Protein phosphatase 1A	8	3
60S ribosomal protein L8	4	3	40S ribosomal protein S27	8	4
Heterogeneous nuclear ribonucleoproteins C1/C2	4	2	E3 ubiquitin-protein ligase CHIP	8	5
Fatty acid synthase	4	3	60S ribosomal protein L23	8	2
Rab GDP dissociation inhibitor beta	3	2	Serine/threonine-protein kinase 38	8	6
40S ribosomal protein S3	3	2	Heat shock protein HSP 90-alpha	7	6
Histone H3.2	3	2	Phosphate carrier protein, mitochondrial	7	4
40S ribosomal protein S8	3	2	Elongation factor Tu, mitochondrial	6	4
Histone H3.1	3	2	Sodium/potassium-transporting ATPase subunit alpha-1	5	5
60S ribosomal protein L19	3	2	ADP/ATP translocase 1	5	4
T-complex protein 1 subunit epsilon	3	2	40S ribosomal protein S2	5	5
T-complex protein 1 subunit alpha	3	3	RNA-binding protein 10	5	4
D-3-phosphoglycerate dehydrogenase	3	3	ATP synthase subunit alpha, mitochondrial	4	4
60S ribosomal protein L10	3	2	Elongation factor 1-alpha 1	4	3
Poly [ADP-ribose] polymerase 1	3	2	DnaJ homolog subfamily A member 1	4	4
Dolichyl-diphosphooligosaccharide-protein glycosyltransferase subunit	3	2	40S ribosomal protein S18	3	3
60S ribosomal protein L23	3	2	Eukaryotic translation initiation factor 4B	3	3
Proliferating cell nuclear antigen	3	3	60S ribosomal protein L10	3	2
Cofilin-1	2	2	26S proteasome non-ATPase regulatory subunit 1	3	3
Eukaryotic initiation factor 4A-II	2	2	BAG family molecular chaperone regulator 5	3	3
ADP/ATP translocase 1	2	2	Sodium/potassium-transporting ATPase subunit alpha-3	2	2
40S ribosomal protein S11	2	2	ATP synthase subunit alpha, mitochondrial	2	2
78 kDa glucose-regulated protein	2	2	40S ribosomal protein S16	2	1
60S ribosomal protein L13	2	2	Methylosome subunit pICln	2	1
Neutral alpha-glucosidase AB	2	2	60S ribosomal protein L11	2	1
40S ribosomal protein S4, X isoform	2	2	OTU domain-containing protein 4	2	2
Ubiquitin-40S ribosomal protein S27a	2	1	Serine/threonine-protein kinase RIO1	2	1
Prohibitin-2	2	2			
Heterogeneous nuclear ribonucleoprotein U	2	2			
60S ribosomal protein L14	2	2			